JOURNAL OF MATERIALS SCIENCE 9 (1974) 359–368

Matrix strengthening in continuous fibre reinforced composites under monotonic and cyclic loading conditions

R. E. LEE, S. J. HARRIS
Department of Metallurgy and Materials Science, University of Nottingham, UK

Unidirectional and cyclic tensile stress-strain testing has been carried out on continuous tungsten fibre reinforced copper composites, with fibre diameter from 11 to 48 μm at a volume fraction of 0.37. In tensile tests the composites showed positive deviations from the rule of mixtures, the amount increasing with a decrease in fibre diameter and, therefore, interfibre spacing. This matrix strengthening continued to failure and was shown to be related in part to the matrix grain size.

In the cyclic stress-strain tests the matrix strengthening was approximately the same for all the composites and was greater than for the tensile tests. The strengthening could be accounted for by the formation of a substructure during cycling of approximately 0.5 μm cell size.

1. Introduction

Observations on metal matrices reinforced with brittle, small diameter, fibres have indicated that failure can take place at lower tensile and cyclic stresses than those predicted by theory [1, 2]. Suggested explanations for such an effect include: (a) the incorporation of weaknesses in the composite during fabrication such as fibre damage and poor fibre-matrix bonding, or (b) the existence of conditions in the composite which prevent the matrix behaving in a ductile manner when associated with certain fibre sizes and distributions.

The rule of mixtures, as expressed by the equation

$$\sigma_c = \sigma_f V_f + \sigma_m{}^1 (1 - V_f) \quad (1)$$

is often used to describe the behaviour of composites under stress. Assuming that the fibre and matrix have equal strain, σ_c, σ_f and $\sigma_m{}^1$ are the stresses in the composite, fibre and matrix, respectively, at any given strain and V_f is the volume fraction of the fibres.

In connection with reason (b) above, several workers [3-5], using monotonic tensile test data, have used Equation 1 to calculate the effective stress carried by the matrix in the composite, and have shown that it may be considerably in excess of the stress in the unsupported matrix for the same strain. In single crystal copper reinforced with tungsten wires, Kelly and Lilholt [3] have shown that the effective matrix stress is greater than that for unreinforced copper, the difference increasing as the volume fraction increases and the fibre diameter decreases. Explanation of this matrix strengthening effect include: the prolonging of elastic behaviour, particularly in the comparatively thin shells of matrix surrounding the fibres [3]; dislocation pile up at the fibres [6]; and overlapping of the stress fields of adjacent fibres [7]. It is possible that the matrix strengthening effect, leading to reduced matrix ductility, combined with the inherent weakness due to fabrication (reason (a) above) may influence the failure mechanism of a composite.

Fractographic studies of fatigue in aluminium reinforced with carbon and boron fibres have indicated that matrix fatigue cracking was largely responsible for failure [2], implying that the cyclic plastic strain in the matrix may be important. The cyclic plastic strain range (Δe_E) for a composite has been predicted by Baker [9] using the equation,

$$\Delta e_p = \frac{2\sigma_c - 2\sigma_y [(E_f/E_m) V_f + (1 - V_f)]}{E_f V_f + U(1 - V_f)} \quad (2)$$

where σ_y is the yield stress of the cyclically

hardened matrix, U is the effective modulus of the yielded matrix and E_f and E_m are the elastic moduli of the fibre and matrix.

Baker [9] and Kelly *et al* [10] have obtained values of σ_y and U to fit into an expression such as Equation 2, assuming the matrix behaviour to be unaffected by the presence of fibres. Such an assumption will not be valid for composites reinforced with small diameter fibres if matrix strengthening effects occur during cyclic stressing.

A large number of materials undergoing high strain fatigue have been shown to obey the Coffin-Manson relationship [8],

$$N_f^{\frac{1}{2}} \Delta e_p = C \quad (3)$$

where N_f is the number of cycles to failure, Δe_p is the plastic strain amplitude and C is a constant. The effect of matrix strengthening in composites under fatigue conditions would be to reduce the value of Δe_p and thereby increase the fatigue life (assuming this to be the only contributory factor).

In the work reported here matrix strengthening has been studied in polycrystalline copper reinforced with tungsten wires with diameters from 10 to 50 μm. The composites were produced by a fabrication route (filament winding – electrodeposition – hot-pressing) similar to that used for carbon fibre reinforced aluminium and nickel. It is possible, therefore, that the copper-tungsten system may contain similar fabrication weaknesses (if any) to those in carbon reinforced aluminium and nickel, and allow it to be used as a model for the interpretation of the behaviour of the more viable composites. This fabrication technique produces a good spatial distribution of the fibres, which can prove difficult in fabrication by the molten matrix infiltration method.

The cyclic stress-strain behaviour of the composites has also been observed to determine whether matrix strengthening does significantly reduce the plastic strain range of the matrix for a given cyclic stress amplitude.

2. Experimental procedure

2.1. Materials

Copper was unidirectionally reinforced with 37 vol % of as-drawn tungsten wire. Five different wire diameters were used from 11 to 48 μm. The diameter of the wire was measured under an optical microscope with an image shearing eyepiece, and the values are given in Table I.

TABLE I Mechanical properties of tungsten wires extracted from composites

Diameter (μm)	UTS (MN m^{-2})	Elongation (%)	Elastic modulus (GN m^{-2})
11 ± 0.3	2773 ± 70	1.3 ± 0.4	341 ± 10
20 ± 0.2	3120 ± 90	1.6 ± 0.6	345 ± 7
30 ± 0.3	2679 ± 60	2.5 ± 0.9	354 ± 7
40 ± 0.4	3124 ± 90	2.6 ± 0.4	340 ± 10
48 ± 0.3	3412 ± 40	3.1 ± 0.2	374 ± 5

The copper matrix was produced by electrodeposition from an acid sulphate bath, containing 188 g litre^{-1} of cupric sulphate and 74 g litre^{-1} of sulphuric acid, at a current density of 200 A m^{-2} at ambient temperature.

2.2. Specimen preparation

Tungsten reinforced copper was fabricated by a process involving filament winding and electrodeposition [11]. The wire was wound on to a stainless steel mandrel at a pre-determined spacing using a coil winding machine. It was then cathodically degreased in sodium hydroxide solution for 10 min, washed and immediately transferred to the plating bath. Copper was plated on to the wire for an appropriate time to give the required volume fraction. During the plating procedure the mandrel was continuously rotated in the plating bath at 20 rpm. This led to a very even, fine grained, deposit of copper on the tungsten wires and mandrel.

The warp sheet produced was stripped from the mandrel, cut up into pieces 100 mm × 12.5 mm with the fibres aligned parallel to the 100 mm side, and then pressed in vacuum at 700° C for 1 h at a pressure of 80 MN m^{-2}. Sufficient warp sheet was used to produce pressed pieces approximately 0.7 mm thick. These pieces were then cut lengthwise into three with a sharp chisel, to give one piece 2.5 mm wide, from which the fibres were subsequently extracted for testing, and two parallel sided pieces 5 mm wide by 100 mm long, for tensile and cyclic testing. In order to grip these specimens for testing, a piece of small bore copper tubing about 3 cm long filled with epoxy resin was flattened on to each end to provide a gripping area. The volume fractions of the composites were checked by weighing a piece of each material, removing the matrix by dissolution and then weighing the remaining fibres. In each case the volume fraction achieved was within 1 % of the desired

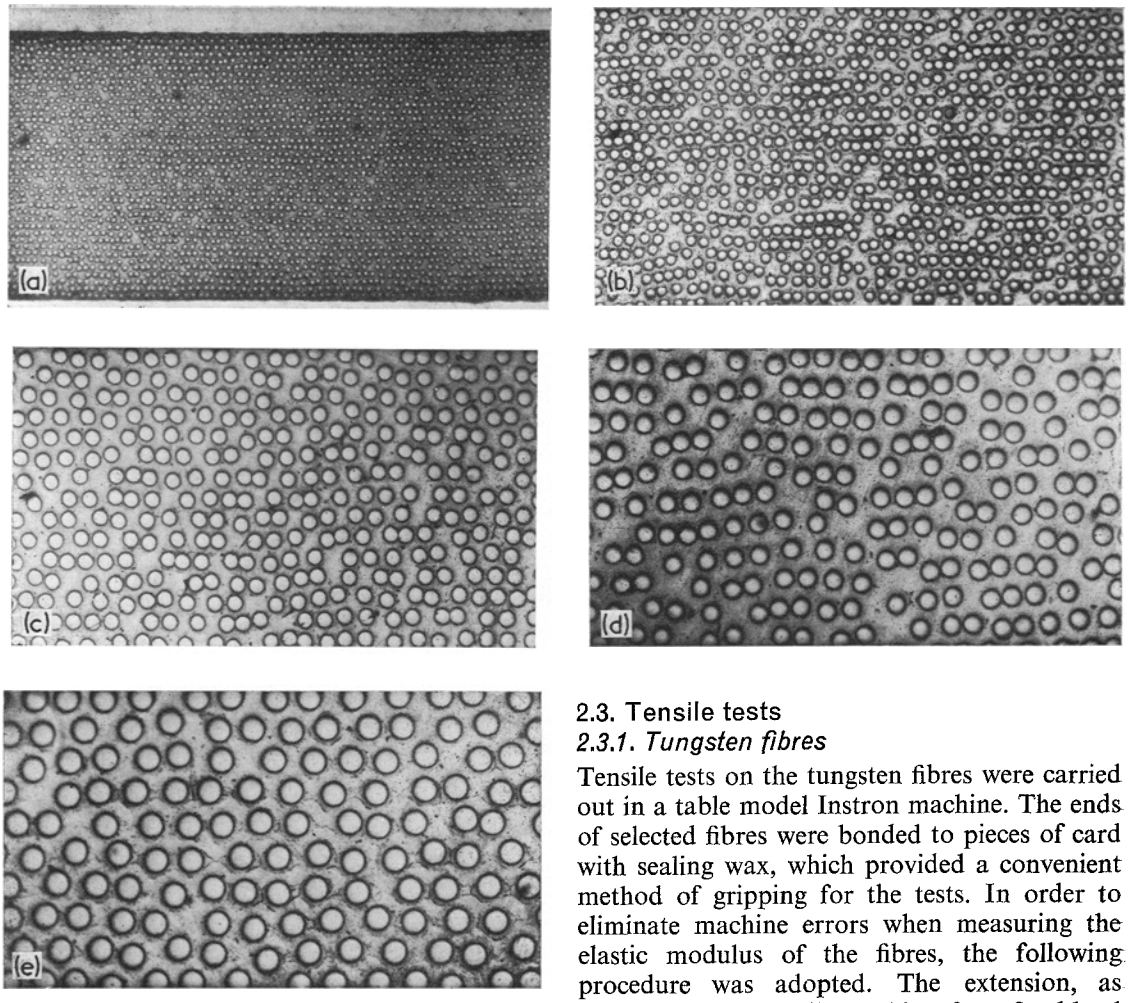

Figure 1 Typical cross-sections through copper-tungsten composites showing good fibre distribution. (a) 11 μm, V_t = 0.36; (b) 20 μm, 0.37; (c) 30 μm, 0.37; (d) 40 μm, 0.37; (e) 48 μm, 0.37.

value. Fig. 1 shows polished cross-sections of typical specimens from the composites produced, demonstrating the very good fibre distribution which can be achieved with the filament winding and electrodeposition process. The dark rings surrounding the fibres in the photograph are due to relief polishing during the preparation of the sections.

Unreinforced copper specimens were made by electrodepositing copper on to the mandrel and then cutting up and hot-pressing a number of layers, as above. The aim was to produce copper specimens by the same process as the composites.

2.3. Tensile tests

2.3.1. Tungsten fibres

Tensile tests on the tungsten fibres were carried out in a table model Instron machine. The ends of selected fibres were bonded to pieces of card with sealing wax, which provided a convenient method of gripping for the tests. In order to eliminate machine errors when measuring the elastic modulus of the fibres, the following procedure was adopted. The extension, as recorded on the tensile machine, for a fixed load was determined for samples of wire with different gauge lengths. A graph of extension against gauge length has a slope whose value is the strain produced in the wire for the given load. Having obtained an accurate value of modulus by this means the strain values were used for normalizing fibre stress-strain curves. This was achieved by scaling the values such that the slope of the initial part of the stress-strain curve gave the correct modulus. This kind of correction was necessary because the fibre strain was taken from the cross-head movement and not directly from the fibre.

2.3.2. Composites

Tensile tests on the composite specimens were carried out in a servo-hydraulic testing machine under load control conditions at a rate of 2.5 kN min^{-1}. Strain in the specimen was measured

with metal foil strain gauges bonded to the surface with Eastman 910 adhesive. Several specimens for each wire diameter were tested to failure and an average stress-strain curve obtained. There was little scatter between measurements from different specimens.

For each pair of composite specimens cut from one pressing some fibres were extracted by dissolution from the thin strip of composite cut from the edge. Ten of these fibres were selected at random and tensile tested whilst a further ten were used for elastic modulus determinations. Average values were obtained in each case. Periodic checks were also made on the fibre diameter. For each pair of specimens the volume fraction of the tungsten in the composite was measured after failure of the specimen. By following this procedure the composite stress-strain curve, average extracted fibre stress-strain curve and fibre volume fraction were obtained for every composite specimen.

The initial portion of the copper stress-strain curve, up to the composite failure strain, was plotted to give a standard curve with which to compare the derived matrix stress-strain curves.

2.4. Cyclic stress-strain tests

In addition to tensile tests cyclic stress-strain tests were carried out on the composites. The specimens were cycled, under load control, from zero stress to a pre-determined stress level until the strain amplitude, as measured by strain gauges, became stable. The stress amplitude was increased (whilst maintaining the minimum value on zero) and the process repeated for a series of stress levels up to failure. Stable hysteresis loops were plotted at each stress level. A cyclic stress-strain curve for each composite was produced by plotting the stress amplitude against the strain amplitude for the hysteresis loops. Once again volume fraction checks were made for each specimen. Cyclic stress-strain curves were also obtained for tungsten fibres extracted from the specimens, and for unreinforced copper.

3. Results

3.1. Unidirectional tensile tests

Fig. 2 shows typical stress-strain curves for tungsten fibres extracted from composites after pressing. The curves in the figure are the mean of ten tests on each fibre diameter. However, little variation in the tensile properties of fibres of a given diameter was observed.

Fig. 3 presents stress-strain curves for as-pressed composites, the fibre diameter being indicated next to each curve. The volume fraction of the 11 μm composites was 0.36, the remaining ones having a volume fraction of 0.37.

Equation 1 may be rearranged to enable the stress on the matrix to be calculated for a given external strain on the composite, the rearrangement being shown in Equation 4.

$$\sigma_m{}^1 = \frac{\sigma_c}{V_m} - \frac{\sigma_f V_f}{V_m} \tag{4}$$

For a given strain σ_c is the stress in the composite measured during the test, σ_f is the stress in the fibre at the same strain, measured on fibres

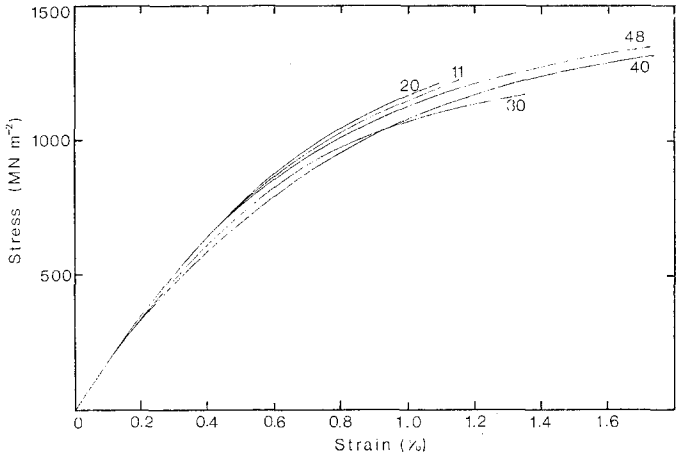

Figure 2 Typical tensile stress-strain curves for copper-tungsten composites. The numbers on the curves refer to the tungsten wire diameters in μm. V_f = 0.37 (0.36 for 11 μm wire composite).

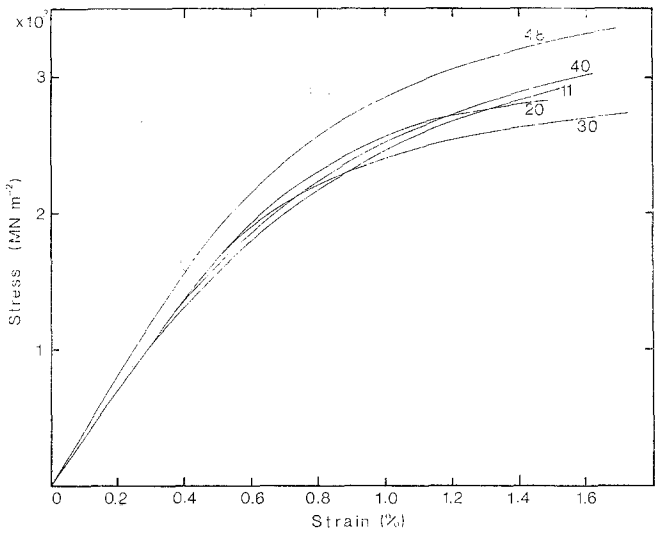

Figure 3 Stress-strain curves for tungsten fibres extracted from pressed copper-tungsten composites. The numbers on the curves are the wire diameters in μm.

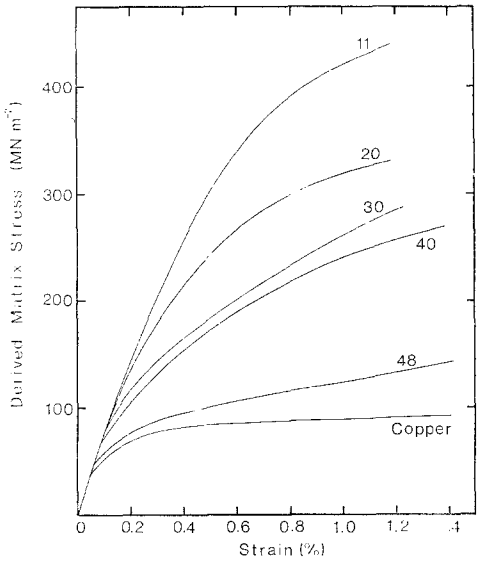

Figure 4 Derived unidirectional stress-strain curves for the matrix in copper-tungsten composites, assuming the rule of mixtures to apply. The stress-strain curve for as-pressed copper is shown for comparison. The numbers are the tungsten wire diameters in μm.

extracted from composites. σ_m^1 is the effective stress acting on the matrix for the rule of mixtures to apply and V_f and V_m are the fibre and matrix volume fractions. Fig. 4 is a plot of σ_m^1 against strain for all the composites, the inherent assumption being that the fibre stress-strain curve is not affected by the fibre being incorporated in a composite. It can be seen that the smaller the fibre diameter (and, therefore, interfibre spacing) the larger is the derived matrix stress value.

The mean breaking strength for the composites is given in Table II. The theoretical values of the breaking stress were calculated for each material using Equation 4 at the failure strain of the composite. The experimental breaking stress exceeded the theoretical values in all cases. The ratio of experimental/theoretical failure strength is shown in Table II and increases with decreasing fibre diameter.

3.2. Cyclic tensile tests

Cyclic stress-strain curves were plotted for all the composites. Using these plots and the cyclic stress-strain curve for extracted tungsten fibres the derived matrix stress under cyclic conditions was calculated from Equation 4. This is plotted against strain in Fig. 5. In the cyclic case the matrix after unloading is put into compression by the elastic contraction of the fibres. This means that during stress cycling of the composite the matrix spends some time in compression and some in tension. In Fig. 5 the axes represent the stress and strain amplitudes suffered by fibres, composite and matrix and do not indicate the levels of the stresses and strain. It can be seen

TABLE II Deviation from rule of mixtures at fracture in copper, tungsten composites

Fibre diameter (μm)	Volume fraction	Composite failure strain (%)	Fibre stress at failure strain (MN m^{-2})	Matrix stress at failure strain (MN m^{-2})	Experimental composite stress at failure (MN m^{-2})	Rule of mixtures composite stress at failure (MN m^{-2})	(Experimental F.S.*/Rule of mixtures F.S.)
11	0.36	1.2	2680	92.5	1206	1024	1.18
20	0.37	1.15	2700	92.0	1210	1056	1.15
30	0.37	1.26	2550	93.5	1100	1002	1.10
40	0.37	1.8	3150	100	1350	1228	1.10
48	0.37	1.75	3350	99	1350	1301	1.04

*F.S. =failure stress

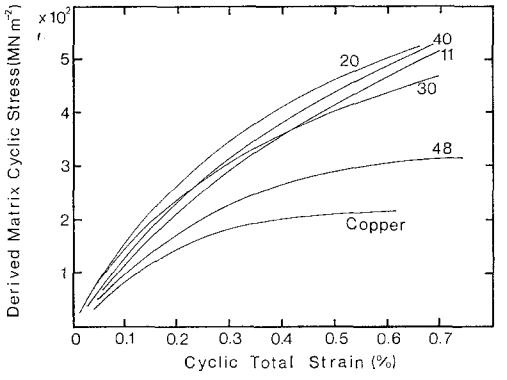

Figure 5 Derived cyclic stress-strain curves for the matrix in copper-tungsten composites, assuming the rule of mixtures to apply. The cyclic stress-strain curve for as-pressed copper is shown for comparison. The numbers are the tungsten wire diameters in μm.

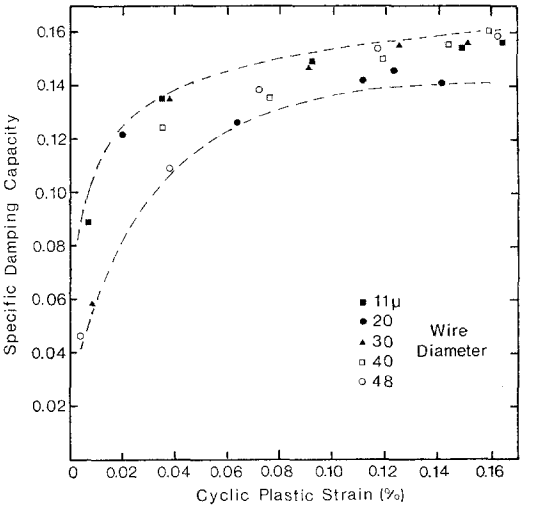

Figure 6 Specific damping capacity plotted against cyclic plastic strain amplitude for copper-tungsten composites. The broken lines indicate the scatter band for the results.

from the figure that the matrix stress-strain curves are much higher than the cyclic curve for unreinforced copper. There are differences between the cyclic and static derived matrix stresses as shown by comparing Figs. 4 and 5. The composites had derived unidirectional matrix stress-strain curves which showed an increasing strength with decreasing fibre diameter for a given volume fraction. In the cyclic case the curves show that the matrix has a stress-strain behaviour in the composite which is of the same order for all fibre diameters but is even harder than the matrix in the unidirectional test.

The areas of the stable hysteresis loops for each composite were measured. From these measurements the specific damping capacity was obtained by taking the ratio of the energy absorbed in the hysteresis loop to the total energy in any load-unload cycle. A plot of specific damping capacity against cyclic plastic strain is given in Fig. 6. There is considerable scatter in the results but they fall within a scatter band determined by the broken lines in Fig. 6 indicating that there is no significant difference between the specific damping capacities of the composites tested. This suggests that as a result of stress-cycling all the composites reach the same stable stress-strain state irrespective of the fibre diameter.

3.3. Metallography

From polished and etched sections through the composites, the grain size of the matrix surrounding the fibres was assessed. Typical examples of these sections are shown in Fig. 7.

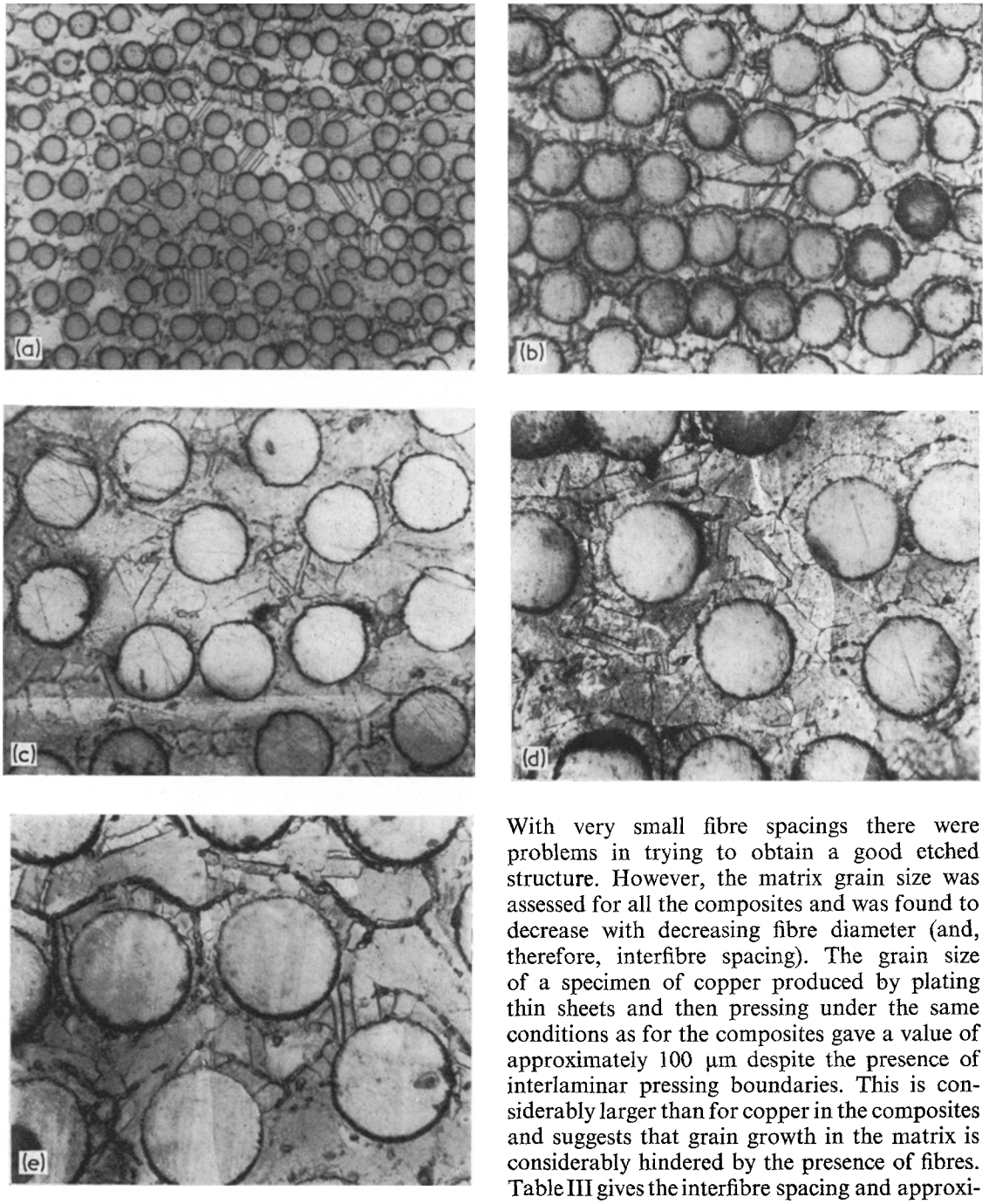

Figure 7 Polished and etched sections of copper-tungsten composites showing the matrix grain size and pressing boundaries. (a) 11 μm, V_f = 0.36; (b) 20 μm, 0.37; (c) 30 μm, 0.37; (d) 40 μm, 0.37; (e) 48 μm, 0.37.

It can be seen that both matrix grain boundaries and interlaminar pressing boundaries show up. With very small fibre spacings there were problems in trying to obtain a good etched structure. However, the matrix grain size was assessed for all the composites and was found to decrease with decreasing fibre diameter (and, therefore, interfibre spacing). The grain size of a specimen of copper produced by plating thin sheets and then pressing under the same conditions as for the composites gave a value of approximately 100 μm despite the presence of interlaminar pressing boundaries. This is considerably larger than for copper in the composites and suggests that grain growth in the matrix is considerably hindered by the presence of fibres. Table III gives the interfibre spacing and approximate matrix grain size for the composites.

4. Discussion

4.1. Matrix monotonic stress-strain behaviour

The results show that the copper matrix in a tungsten fibre reinforced copper composite of

TABLE III Matrix proof stress as a function of fibre diameter and spacing

Fibre diameter (μm)	Interfibre spacing (μm)	Approximate matrix grain size (μm)	Matrix 0.1% proof stress (MN m^{-2})
11	6.5	1.5	175
20	11.8	3	140
30	17.7	4.5	120
40	23.6	6	100
48	28.3	7	80

$V_f \simeq 0.37$ has a matrix stress which increases as the fibre diameter decreases.

There are two types of mechanism which have been put forward in the literature to account for this effect. The first is one of dislocation extrusion and pile-up, where dislocations in the matrix are influenced by the presence of grain boundaries and fibre-matrix interfaces. The second effect is concerned with the triaxial stresses which can be generated in the composites due to differences in the Poisson's ratio for the two phases. These stresses have the effect of inhibiting matrix-yielding.

The first of these mechanisms is similar to that described by Petch and Hall in which the yield point of a material is a function of the grain size. This is expressed in the form:

$$\sigma_y = \sigma_0 + k(l)^{-\frac{1}{2}} \quad (5)$$

where σ_y is the yield stress, l is the grain diameter and σ_0 and k are constants. In terms of a proof stress, which was measured in the present experiments (see Table III), the Petch-Hall relationship then represents the stress necessary to produce a given plastic strain in the material. Any obstacle such as a grain boundary or fibre-matrix interface presents a barrier to dislocation motion, the number and strength of such barriers being reflected in the proof stress value.

In the present experiments it was observed that the detectable matrix grain size was a function of the fibre diameter and, therefore, interfibre spacing, reducing as the latter decreased. It seemed justified, therefore, to look for an explanation of the increasing proof stress in terms of a Petch type relationship, with respect to the matrix grain size.

In Fig. 8 the filled circles are the experimentally determined values of the 0.1% proof stress plotted against the interfibre spacing. Line A is the result of applying the Petch equation using the observed matrix grain size and value of the constants σ_0 and k of 25 MN m^{-2} and 0.11 MN m$^{-3/2}$ obtained from the literature for polycrystalline copper [4]. It can be seen that this analysis considerably underestimates the observed 0.1% proof stress values. Even taking into account uncertainty in the values of σ_0 and k, it is not possible to fit the Petch equation to the results using the observed matrix grain size. On the other hand, line B shows the result of fitting the Petch equation to the results by selecting an appropriate value of grain diameter. A reasonable fit is achieved by taking the grain diameter in the matrix to be 1/12 of the interfibre spacing, which is a factor of 3 lower than experimentally observed. The numerical difference between the experimental proof stress values and those predicted theoretically in curve A, gradually increases with decreasing fibre spacing, suggesting that the difference might be accounted for in terms of an additional mechanism.

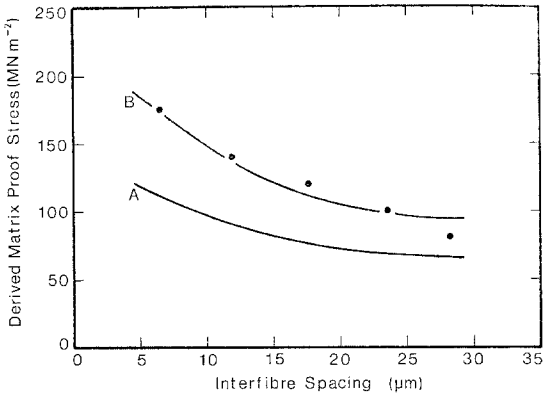

Figure 8 A plot of derived matrix 0.1% proof stress against interfibre spacing for copper-tungsten composites. The filled circles represent the experimental points. Lines A and B are theoretical lines obtained by applying the Petch relationship; A to the observed matrix grain size and B to an apparent grain size needed to fit the experimental points.

This mechanism may be that proposed by Kelly and Lilholt [3] in their study of 10 and 20 μm diameter tungsten wires in a cast copper matrix. They suggest that triaxial stresses are built up in a proportion of the matrix due to Poisson's ratio differences between the elastic fibre and the plastic matrix. They expressed this in terms of the slope of the matrix stress-strain curve immediately after the yield of the matrix. The expression is of the form:

$$\frac{d\sigma}{de} = \frac{V_f(1 - 2\nu_f)^2}{(V_f/k_m) + (V_m/k_{pf}) + (1/G_f)} \quad (6)$$

where V_f is Poisson's ratio for the fibres, K_m is the matrix bulk modulus. k_{pf} is the plane strain bulk modulus for the fibres, G_f is the fibre shear modulus and V_f and V_m are the fibre and matrix volume fractions. It is seen that the slope depends only on the volume fraction for a composite with given components. This means that the contribution this effect makes to the 0.1% proof stress for the present composites should be constant, depending only on volume fraction. This was not the case for the results reported here, the stress which must be added to line A to take it up to the experimental points, increasing from 15 MN m^{-2} at 28 μm spacing to 60 MN m^{-2} at 6.5 μm spacing.

In some of Kelly and Lilholt's experiments the matrix stress began to drop when the fibres reached their yield strain, which was attributed to release of the constraint on the matrix because the fibre and matrix Poisson's ratios became approximately equal. No such behaviour was observed in the present experiments and, in fact, the matrix stress continued to rise even after the fibres yielded. This suggests that the enhancement of the matrix stress is not due to a triaxial constraint effect. However, it is difficult to explain the difference between the observed values and those predicted from the Petch equation using the measured grain size.

A clue may come from the cyclic stress-strain experiments reported here. It was found that as a result of stress cycling the matrix 0.1% proof stress was approximately the same value for all the composites. It is known that on stress cycling materials a dislocation substructure builds up which has dimensions independent of grain size. This suggests that the matrix proof stress values may fit a Petch type relationship with the grain size replaced by the substructure size. The substructure size required to achieve such a fit is approximately 0.5 μm which is close to that observed in copper after stress cycling by Grosskreutz [12].

The fact that the existence of a substructure could explain the cyclic stress-strain behaviour of the matrix suggests that the poor fit of the Petch relationship for the monotonic test could be improved by postulating the existence of a substructure or other dislocation blocking mechanism in as-pressed composites. A possible source of this is from the stresses induced in the matrix by the differential contraction of the tungsten and copper on cooling from the pressing temperature (700°C) due to the differences in the thermal expansion coefficients (tungsten = 4.5×10^{-6} °C^{-1}, copper = 16.5×10^{-6} °C^{-1}). Hancock and Grosskreutz [13] working with stainless steel reinforced aluminium composites found that quite extensive dislocation structures were observed after rapidly cooling from 500°C. The dislocation density was highest in a zone approximately 20 μm thick around each fibre. They attributed this to differential thermal contraction. Chawla [14], working with large tungsten fibres in a single crystal copper matrix also observed considerable amounts of slip as a result of thermal cycling, the dislocation density being highest in the region close to the fibres.

The elastic transverse radial stress σ_r at the fibre-matrix interface is given approximately by:

$$\sigma_r = E_m (\alpha_f - \alpha_m) \Delta T \qquad (7)$$

where E_m is the elastic modulus of the matrix, α_f and α_m are the linear coefficients of thermal expansion of the filament and matrix and ΔT is the temperature interval. For copper-tungsten σ_r = 1000 MN m^{-2} which is considerably in excess of the UTS for copper of 220 MN m^{-2}. This stress does not, of course, develop in the matrix, but the process will lead to the production of a large number of dislocations within the matrix. The degree of interaction between the dislocation stress field around each fibre will be greatest at small interfibre spacings, and may lead to a high level of matrix work hardening. This effect may, in part, be responsible for the matrix strengthening effects observed in the present composites.

4.2. Breaking strength of composites

As mentioned earlier, the derived matrix stress did not fall after the fibres yielded, but continued to rise right up to failure, leading to composite fracture stresses in excess of those predicted by the rule of mixtures. Such a result indicated that the relatively poor bonding, (i) between fibre and matrix, (ii) between the monolayer sheets in this type of material obtained using the filament winding – electroplating – hot-pressing fabrication route, does not impair the strength of the composites. In using copper-tungsten as a model for systems such as aluminium-carbon, it should be remembered that carbon fibres do not possess the small amount of ductility found in tungsten fibres and also the diffusion bonding of aluminium/carbon monolayer sheets is more difficult than that of copper/

tungsten due to the tenacious oxide coating on aluminium. It is likely, therefore, that failure of aluminium/carbon at stresses below rule of mixtures results from fibre damage and degradation during fabrication, which was not observed with tungsten.

4.3. Relevance of cyclic tests to fatigue behaviour

The higher effective cyclic work hardening rate which has been measured in all the above composites indicates that both σ_y and U in Equation 2 are effectively increased. This means that the plastic strain range Δe_p will be reduced. If the Manson-Coffin relation is obeyed this should lead to an increase in life during high strain fatigue. The results appear to show that the cyclic work-hardening rate is not so dependent on fibre spacing as the monotonic hardening rate (see Figs. 5 and 6).

It is worth noting in Fig. 5 that the 48 μm fibre composite cyclically hardened to a level between that of pure copper and the remaining composites. The majority of the fatigue data on composites appearing in the literature has been obtained for materials in which the fibre diameters exceed 48 μm. Hence, the effect of fibre diameter has not been explored in the size range where the highest levels of work-hardening are to be expected, one exception is the work carried out on carbon-aluminium [2], where poor fatigue lives were obtained.

Acknowledgements

The authors are indebted to the Science Research Council for providing finance to support this work. They would like to extend their thanks to Professor J. S. Ll. Leach for providing laboratory facilities and to Mr C. E. Jagger for preparing the materials for this investigation.

References

1. P. JACKSON, D. M. BRADDICK and A. A. BAKER, *Fibre Sci. & Tech.* **5** (1972) 219.
2. A. A. BAKER, D. M. BRADDICK and P. JACKSON, *J. Mater. Sci.* **7** (1972) 747.
3. A. KELLY and H. LILHOLT, *Phil. Mag.* **20** (1969) 311.
4. E. GARMONG and L. A. SHEPARD, *Met. Trans.* **2** (1971) 175.
5. W. F. STUHRKE, ASTM STP 438 (1969) p. 108.
6. P. NEUMANN and P. HAASEN, *Phil. Mag.* **23** (1971) 285.
7. K. TANAKA and T. MORI, *ibid* **23** (1971) 737.
8. J. F. TAVERNELLI and L. F. COFFIN, *Trans. ASM* **51** (1959) 438.
9. A. A. BAKER, *Appl. Mat. Res.* **5** (1966) 143.
10. A. KELLY and M. J. BOMFORD, "Physics of Strength and Plasticity" (M.I.T. Press, Cambridge, Massachusetts, 1969) p. 339.
11. A. A. BAKER, A. MARTIN and R. J. BACHE, "Composites", **2** (1971) 154.
12. J. C. GROSSKREUTZ, "Fatigue *I* An Interdisciplinary Approach", edited by J. J. Burke (Syracuse N.Y. University Press, 1964) p. 27.
13. J. R. HANCOCK and J. C. GROSSKREUTZ, ASTM STP 438 (1969) p. 134.
14. K. K. CHAWLA, *Metallography* **6** (1973) 155.

Received 13 September and accepted 5 October 1973.